

Oxidative potential in rural, suburban and city centre atmospheric environments in Central Europe

Máté VÖRÖSMARTY¹, Gaëlle UZU², Jean-Luc JAFFREZO², Pamela DOMINUTTI²,
Zsófia KERTÉSZ³, Enikő PAPP³, and Imre SALMA⁴

¹ Hevesy György Ph. D. School of Chemistry, Eötvös Loránd University, Budapest, Hungary

² University of Grenoble Alps, IRD, CNRS, INRAE, Grenoble, France

³ Laboratory for Heritage Science, Institute for Nuclear Research, Debrecen, Hungary

⁴ Institute of Chemistry, Eötvös Loránd University, Budapest, Hungary

Correspondence to: Imre Salma (salma.imre@ttk.elte.hu)

Abstract. Oxidative potential (OP) is an emerging health-related metric which integrates several physicochemical properties of particulate matter (PM) that are involved in the pathogenesis of the diseases resulting from the exposure to PM. Daily PM_{2.5}-fraction aerosol samples collected in the rural background of the Carpathian Basin and in the suburban area and centre of its largest city of Budapest in each season over one year were utilised to study the OP at the related locations for the first time. The samples were analysed for particulate matter mass, main carbonaceous species, levoglucosan and 20 chemical elements. The resulted data sets were subjected to positive matrix factorisation to derive the main aerosol sources. Biomass burning (BB), suspended dust, road traffic, oil combustion, vehicle metal wear and mixed industrial source were identified. The OP of the sample extracts in simulated lung fluid was determined by ascorbic acid (AA) and dithiothreitol (DTT) assays. The comparison of the OP data sets revealed some differences in the sensitivities of the assays. In the heating period, both the OP and PM mass levels were higher than in spring and summer, but there was a clear misalignment between them. In addition, the heating period-to-non-heating period OP ratios in the urban locations were larger than for the rural background by factors of 2–4. The OP data sets were attributed to the main aerosol sources using multiple linear regression with the weighted least squares approach. The OP was unambiguously dominated by BB at all sampling locations in winter and autumn. The joint effects of motor vehicles involving the road traffic and vehicle metal wear played the most important role in summer and spring, with considerable contributions from oil combustion and resuspended dust. In winter, there is temporal coincidence between the most severe daily PM health limit exceedances in the whole Carpathian Basin and the chemical PM composition causing larger OP. Similarly, in spring and summer, there is a spatial coincidence in Budapest between the urban hotspots of OP-active aerosol constituents from traffic and the high population density in central quarters. These features offer possibilities for more efficient season-specific air quality regulations focusing on well-selected aerosol sources or experimentally determined OP rather than on PM mass in general.

34 **1 Introduction and objectives**

35 Poor air quality caused by high concentrations of particulate matter (PM) is one of the most severe public
36 health concerns for humans worldwide (e.g. Lelieveld et al., 2015, 2020; Bondy, 2016; Cohen et al.,
37 2017). Its acute and chronic effects, such as lung, cardiovascular and cerebrovascular diseases have been
38 documented in both epidemiological and toxicological studies (e.g. Donaldson et al., 2005; Valavanidis
39 et al., 2008; Apte et al., 2015; Riediker et al., 2019; Kelly and Fussell, 2020).

40

41 Due to the chemical, physical and biological complexity of ambient aerosol particles, their dynamic
42 character and possible synergisms among air pollutants, a sophisticated interplay of multiple factors is
43 involved in the pathogenesis of the diseases resulting from the exposure to PM. The main factors can
44 involve: 1) mass concentrations of PM_{2.5} or PM₁₀ size fractions, 2) amounts of potentially toxic chemical
45 components such as transition and heavy metals, polycyclic aromatic hydrocarbons (PAHs), soot and
46 specific organics, 3) certain chemical speciation forms such as Cr(VI) versus Cr(III), 4) lung
47 bioaccessibility of critical constituents, 5) surface reactivity of particles, 6) number concentrations of very
48 small particles such as ultrafine particles or engineered nanomaterials, 7) shape and morphology of
49 particles such as for asbestos or silica and 8) active components of biogenic origin such as bacteria,
50 viruses, pollens and moulds or with radioactivity such as radon progeny (Riediker et al., 2019). Therefore,
51 it cannot be expected that a single or a few aerosol metrics broadly express the induced biological
52 responses. In the first approximation, PM mass is often selected from these factors as a simplistic metric,
53 and it can be refined by further particle properties.

54

55 One of the most important biological mechanisms by which PM induces adverse health effects is causing
56 an oxidant-antioxidant imbalance in the respiratory system at the cellular level (Kelly and Mudway, 2003;
57 Borm et al., 2007; Kelly and Fussell, 2012, 2015; Cassee et al., 2013; Valavanidis et al., 2013; Janssen et
58 al., 2014). This is called as oxidative stress. It is related to 1) stimulating cells to uncontrolled production
59 of excess reactive oxygen species (ROS) endogenously, e.g. directly by Fenton-type reactions of redox-
60 active aerosol components in the human body or indirectly through biotransformation, e.g. of PAHs or 2)
61 inefficient elimination of ROS by the antioxidant defence system of the body. These can lead to
62 inflammatory processes that increase the risk for various diseases and can result in biological aging and
63 apoptosis (Ayres et al., 2008; Verma et al., 2012; Gao et al., 2020). The capacity of PM to invoke oxidative
64 stress is quantified by its oxidative potential (OP). This integrates several factors of the particle properties
65 1–8 listed above. Numerous epidemiological studies suggest that the OP can be one of the central
66 quantities that is responsible for several health endpoints including specific acute ~~health~~-effects such as

67 emergency treatment of asthma and congestive heart failure and that largely explains the underlying
68 biological bases of toxicity (e.g. Bates et al., 2015; Kelly and Fussel, 2015; Abrams et al., 2017; Yue et
69 al., 2018; [Weichenthal et al., 2019](#); Daellenbach et al., 2020; Dhalla et al., 2000; Zhang et al., 2022;
70 Baumann et al., 2023).

71

72 As a result, there has been a substantial and increasing scientific interest in the measurement
73 improvements of OP using (biological) in vivo, in vitro cellular and in vitro acellular assays, and in the
74 identification of the aerosol components and sources closely related to OP (e.g. Cho et al., 2005; Künzli
75 et al., 2006; Boogaard et al., 2012; Verma et al., 2014, 2015; Kelly and Fussel, 2015; Fang et al., 2016;
76 Calas et al., 2017; Weber et al., 2018; Shahpoury et al., 2021; Borlaza et al., 2021b, 2022; Lionetto et al.,
77 2021; Zhang et al., 2022). The OP is frequently measured by acellular assays for exogenous ROS, in
78 which the PM extract or the particles directly cause a consumption rate of some antioxidants such as
79 ascorbic acid (AA) or of some chemical surrogates to cellular reducing agents, e.g. dithiothreitol (DTT).
80 The quantifications are generally based on spectrophotometry. More sophisticated detection methods
81 which directly determine the ROS production are also available (Katerji et al., 2019).

82

83 The most frequently used assays were compared for PM₁₀-fraction aerosol samples considering the
84 chemical composition of particles as well (Calas et al., 2018; Lionetto et al., 2021; [Shahpoury et al.,
85 2022](#)). It was concluded that the assays correlated with each other but were not equivalent. All assays
86 were somewhat specific, and no consensus has been reached on the “best assay” nor on a standardised
87 methodology for each assay (Weber et al., 2021; Zhang et al., 2022). [At the same time, it seems sensible
88 to compare the results obtained by an identical sample preparation and OP measurement method for
89 different environmental types. Likewise, comparing the data derived by different experimental methods
90 applied to similar sample types can contribute to revealing and understanding the different properties or
91 characteristics of these methods for various chemical components and sources. Both approaches can also
92 yield considerable methodological development.](#)

93

94 The main common features of the assays are that 1) they exhibit different responses to various groups of
95 ROS-generating compounds and their bioavailability, 2) their sensitivity depends on the partner reaction
96 compound to ROS, and 3) they show nonlinear response to PM mass concentration (Charrier et al., 2016;
97 Fang et al., 2016; Calas et al., 2017; Shahpoury et al., 2021). A large number of PM constituents were
98 identified to influence the OP. The DTT assay responds sensitively to ROS produced by organic
99 compounds and indirectly by soluble transition metals, mainly Cu(II), Mn(II) and Fe(II), and can be also
100 influenced by synergetic or antagonistic effects between some chemical components (Charrier and

101 Anastasio, 2012; Bates et al., 2019; Shahpoury et al., 2021; Borlaza et al., 2022). The AA assay was
102 shown to express large sensitivity to transition metals and some specific organics such as quinones
103 (Künzli et al., 2006; Godri et al., 2011; Visentin et al., 2016).

104

105 It is important to extend the studies on this emerging health-related metric to cities and regions in the
106 world. The knowledge on the OP for a large part of Central Europe, namely the Carpathian Basin, is
107 deficient or missing (Szigeti et al., 2015). The major objective of this study was to present, discuss and
108 interpreted the OP data determined by AA and DTT assays in PM_{2.5}-fraction aerosol samples collected in
109 parallel in central Budapest, its suburban area and rural background within the Carpathian Basin in each
110 season over one year. We also investigated the spatiotemporal dependencies, and identified the main
111 aerosol sources of OP. The study can contribute to our general knowledge on the OP as well.

112 **2 Methods**

113 **2.1 Sample collections**

114 The samplings in the rural background were performed at the K-puszta station (N 46° 57' 56", E 19° 32'
115 42", 125 m above sea level, a.s.l.), which represents the main plain part of the basin (Salma et al., 2020a).
116 Budapest, with ca. 2.2 million inhabitants in the metropolitan area, is the largest city in the region. Its
117 suburban environment was characterised by collections at the Marczell György Main Observatory (N 47°
118 25' 46", E 19°10' 54", 138 m a.s.l.) of the Hungarian Meteorological Service (Salma et al., 2022). This is
119 in a southeast residential part of the city. The samplings in the city centre were accomplished at the
120 Budapest platform for Aerosol Research and Training (BpART) Laboratory (N 47° 28' 30", E 19° 03' 45",
121 115 m a.s.l.), which represents an average atmosphere of the city centre (Salma et al., 2016).

122

123 Three identical high-volume sampling devices equipped with PM_{2.5} inlets (DHA-80, Digitel, Switzerland)
124 were deployed at the sites (Salma et al., 2020a). The collection substrates were prebaked quartz fibre
125 filters with a diameter of 150 mm (QR-100, Advantec, Japan). Daily aerosol samples were taken starting
126 at midnight of local time. The samples corresponding to air volumes of 720 m³ were collected in parallel
127 with each other over semi-consecutive days in October 2017 (autumn), January 2018 (winter), April 2018
128 (spring) and July 2018 (summer). The total numbers of the filters were 56 in the rural background, 59 in
129 the suburban area, and 28 in the city centre. The samples evenly spread among the four seasons. In
130 addition, one field blank was taken at each location and in each season. The filters were wrapped in
131 preheated Al foils, sealed in plastic bags and stored at a temperature of <-4 °C until the analyses. The

132 samples represent a gradual transition from the central part of a large continental European city through
133 its suburban area to its regional background in all seasons.

134 **2.2 Analyses and data treatment**

135 Particulate matter mass was determined by gravimetry (Cubis MSA225S-000-DA, Sartorius, Germany,
136 sensitivity of 10 μg). The blank-corrected PM mass data were above the limit of quantitation (LOQ),
137 which was 1 $\mu\text{g m}^{-3}$ (Salma et al., 2022).

138

139 Filter punches were analysed by thermal-optical transmission method using a laboratory OC/EC analyser
140 (Sunset Laboratory, USA) adopting the EUSAAR-2 thermal protocol (Cavalli et al., 2010). All blank-
141 corrected organic carbon (OC) and elemental carbon (EC) data were above the LOQ, which were 0.38
142 and 0.04 $\mu\text{g m}^{-3}$, respectively. Filter pieces were analysed for levoglucosan (LVG) by gas
143 chromatography–mass spectrometry (Varian 4000, USA) after trimethylsilylation (Blumberger et al.,
144 2019). All blank-corrected LVG data were above the LOQ, which was 1.2 ng m^{-3} .

145

146 Parts of the filters were analysed by particle-induced X-ray emission spectrometry for S, Cl, K, Ca, Ti,
147 V, Cr, Mn, Fe, Co, Ni, Cu, Zn, As, Br, Rb, Sr, Zr, Ba and Pb using an external beam of protons with an
148 energy of 2.35 MeV and a current of 20 nA (Aljboor et al., 2022). The obtained spectra were evaluated
149 by the GUPIXWIN program. The filters were treated as thin layer samples. For S, Cl, K, Ca, the self-
150 absorption effects of quartz filters were corrected for (Chiari et al., 2018). The lung bioaccessibility was
151 assessed in the present work by the total amounts of the chemical species as the first approximation.

152

153 Concentrations of EC and OC from fossil fuel combustion and from biomass burning (BB), namely EC_{FF}
154 and OC_{FF} , EC_{BB} and OC_{BB} , respectively and of OC from biogenic sources (OC_{BIO}) were previously
155 estimated by a coupled radiocarbon-LVG marker method (Salma et al., 2020a). Secondary organic carbon
156 (SOC) was also assessed previously using the EC tracer method for primary OC (Salma et al., 2022).
157 These results were used as supplementary data in interpretations.

158 **2.3 Determination of oxidative potential**

159 Specified filter areas were extracted in a simulated human respiratory tract lining fluid solution composed
160 of Gamble's solution with dipalmitoylphosphatidylcholine (DPPC; the major phospholipid of lung
161 surfactant; Calas et al., 2017, 2018). The extractions were carried out by vortex agitation at 37 °C for 1
162 h. The overall procedure represents conditions which are close to the respiratory system. Isoconcentration

163 extracts with $10 \mu\text{g ml}^{-1}$ of PM mass were obtained for all samples to overcome possible nonlinear OP
164 response of PM concentrations (Charrier and Anastasio, 2012; Calas et al., 2017).

165

166 The ~~OP of the sample~~ extracts ~~were not filtered, so they contained insoluble chemical species including~~
167 ~~those with active surface area (Baumann et al., 2023). The OP~~ was measured ~~without filtration~~ by two
168 single-compound in vitro acellular assays, i.e. AA and DTT assays. These two methods are widely used
169 for OP determination (e.g. Calas et al., 2018; Daellenbach et al., 2020; Lionetto et al., 2021; Shahpoury
170 et al., 2021, 2022). However, there is a fundamental difference between them regarding their underlying
171 chemical mechanisms (Charrier and Anastasio, 2012). The quantifications were based on plate-reader
172 spectrophotometry (Tecan Infinite M200 Pro, Switzerland) in MilliQ water for AA, and in a phosphate
173 buffer with a physiological pH value of 7.4 after adding 5,5'-dithiobis(2-nitrobenzoic acid), with readings
174 taken at different specified reaction times (Calas et al., 2018; Borlaza et al., 2021b, 2022). The possible
175 transition metal contamination of the buffer was removed by Chelex 100 resin to reduce the background
176 oxidation. The consumption rates of the AA or DTT were obtained from the simple linear regression of
177 the absorbance values in time at 265 and 412 nm, respectively. The coefficients of determination R^2 for
178 the regression were >0.90 when $<70\%$ of the initial amount of the reagent was oxidised. Matrix
179 absorbance was considered, and the quality assurance of the determinations was performed by positive
180 control tests (Borlaza et al., 2021b). The limits of detection (LODs) for the AA and DTT assays were set
181 at three times the standard deviation (SD) for the blank extracts and were typically 0.008 and 0.0014 nmol
182 min^{-1} , respectively. The experimental protocols were described in more detail previously (Calas et al.,
183 2017, 2018).

184

185 The OP data measured by the AA and DTT assays were normalised to $\text{PM}_{2.5}$ mass (m) or sampled air
186 volume (V) and are denoted as $\text{OP}_{\text{AA},m}$, $\text{OP}_{\text{DTT},m}$, $\text{OP}_{\text{AA},V}$ and $\text{OP}_{\text{DTT},V}$. The consumption rates normalized
187 to V are often considered to have a closer relationship to human exposure, while those normalized by m
188 are regarded as a measure of the inherent ~~toxicity~~ OP of PM (Weber et al., 2018; Yu et al., 2019).

189 **2.4 Mathematical models**

190 Source apportionment modelling was accomplished to identify and quantify the main aerosol sources
191 using positive matrix factorisation (PMF, US Environmental Protection Agency, version 5.0; EPA, 2017).
192 It decomposes the sample data matrix into a linear combination of two matrices: a daily factor contribution
193 varying in time and factor profiles by minimizing the critical compound parameter Q (Paatero and Tapper,
194 1994; Hopke, 2016, 2000). The input data set contained the concentrations and uncertainties of $\text{PM}_{2.5}$
195 mass, S, Cl, K, Ca, Ti, V, Cr, Mn, Fe, Ni, Cu, Zn, Br, Rb, Ba, Pb, EC, OC and LVG for all sampling sites

196 and seasons. A multisite PMF modelling with 143 samples was performed (Dai et al., 2020). For most
197 chemical species, all concentrations were higher than the LODs. For some trace elements, the
198 concentrations were larger than the LODs in >60 % of the samples. The missing data were replaced by
199 the related median with an uncertainty of 5/6 of the LOD value. The concentrations above LODs were
200 associated with an equation-based extra standard deviation in accordance with the guidelines of the PMF
201 manual, which involved the measurement uncertainty, the concentration and the LOD values (EPA,
202 2017). Elements Cl, Cr, Ni and Rb were specified as weak variables due to their relatively large SDs.

203

204 Several test runs were performed with a total number of factors ranging from 3 to 9 to define the base
205 runs. To explore the goodness of the individual results and to derive robust source apportionment,
206 additional mathematical tools such as bootstrapping and displacement methods were adopted (Norris et
207 al., 2014). In bootstrapping, the compliance between the base factors and bootstrapped factors (which
208 were later selected as the final solution) was >80 %. In addition, the displacement for these solutions did
209 not show larger changes in the parameter Q and no swap counts of factors occurred.

210

211 Multiple linear regression (MLR) modelling was performed to deconvolute the measured $OP_{AA,V}$ and
212 $OP_{DTT,V}$ data sets as the dependent variables among the main aerosol sources identified by the PMF as the
213 independent variables (Weber et al., 2021). A linear predictor function was fitted through the dependent
214 variable points by the weighted least squares (WLS) method. The weights were chosen as the inverse of
215 the square of the SD for each measured OP. Goodness of the fit was checked by residual analysis. The
216 significant predictor variables were selected using an *F*-test. The calculations were performed in the
217 advanced analytics software package Statistica (version 7.1, StatSoft, Germany).

218 **3 Results and discussion**

219 **3.1 Ranges, averages and tendencies**

220 Basic statistics of the daily OP data and atmospheric concentrations obtained from the filters for the whole
221 sampling interval in the three environments are summarised in Table 1. Some further atmospheric
222 concentrations measured online and the local meteorological data together with their measuring methods
223 are given in Sect. S1 in the Supplement. The concentrations of EC_{FF} , OC_{FF} , EC_{BB} , OC_{BB} , OC_{BIO} and SOC
224 derived earlier can be found in previous publications (Salma et al. 2020a, 2022). The present average
225 concentrations and meteorological data are in line with the results of earlier studies (Salma et al., 2004,
226 2005, 2020a; Szigeti et al., 2015) suggesting that the overall data set represents typical atmospheric
227 conditions at the locations. However, several Saharan dust intrusions into the Carpathian Basin happened

228 in April 2018 (Varga, 2020). The most intensive event reached the region via southern Italy and the
 229 Balkans on 15 April and affected the studied region for a few days.

230

231 **Table 1.** Ranges and medians of oxidative potential (OP) determined by AA and DTT assays and normalised to PM mass (m ;
 232 $OP_{AA,m}$ and $OP_{DTT,m}$, respectively, in unit of $\text{nmol min}^{-1} \mu\text{g}^{-1}$) or to sampled air volume (V ; $OP_{AA,V}$ and $OP_{DTT,V}$, respectively,
 233 $\text{nmol min}^{-1} \text{m}^{-3}$), of concentrations for $\text{PM}_{2.5}$ mass ($\mu\text{g m}^{-3}$), chemical elements (all in ng m^{-3}), elemental carbon (EC), organic
 234 carbon (OC, both in $\mu\text{g m}^{-3}$), levoglucosan (LVG, ng m^{-3}) in the rural background, suburban area and city centre.

235

Site/ Variable	Rural background			Suburban area			City centre		
	Minimum	Median	Maximum	Minimum	Median	Maximum	Minimum	Median	Maximum
$OP_{AA,m}$	0.01	0.12	0.28	0.02	0.14	0.33	0.03	0.11	0.23
$OP_{AA,V}$	0.1	1.5	5.2	0.3	2.4	11.7	0.3	2.1	4.9
$OP_{DTT,m}$	0.04	0.10	0.20	0.004	0.11	0.27	0.11	0.17	0.27
$OP_{DTT,V}$	0.3	1.2	3.1	0.03	1.9	6.2	1.3	2.9	6.1
$\text{PM}_{2.5}$	6	14	29	7	18	46	7	18	44
S	51	311	1043	84	312	823	167	367	952
Cl	5	11	28	5	32	118	5	23	71
K	11	56	234	9	65	363	18	91	264
Ca	1	33	215	6	73	457	23	104	468
Ti	0.05	1.3	15	0.3	1.9	26	0.6	3.1	22
V	0.23	0.46	1.1	0.13	0.43	1.0	0.13	0.44	1.2
Cr	0.16	0.37	0.91	0.18	0.46	1.7	0.17	0.76	7.2
Mn	0.4	2.0	16	0.1	2.1	5.6	0.5	3.3	11
Fe	5	32	162	16	63	306	33	102	607
Ni	0.13	0.42	1.3	0.14	0.33	1.1	0.18	0.57	3.0
Cu	0.13	0.94	6.8	0.6	1.6	7.5	0.8	2.9	27
Zn	0.9	7.2	40	3	12	53	1	17	48
Br	0.20	0.77	3.0	0.2	1.2	4.1	0.5	1.3	2.7
Rb	0.22	0.35	0.76	0.22	0.36	0.83	0.24	0.34	0.80
Ba	1.1	2.4	12	1.1	3.1	12	1.1	4.5	13
Pb	0.6	3.4	28	1.5	5.3	21	1.3	5.6	19
EC	0.08	0.22	0.77	0.21	0.50	1.1	0.31	0.78	1.8
OC	0.9	2.3	6.0	1.0	2.9	11	2.0	3.3	8.0
LVG	4	38	776	5	106	1765	8	203	709

236

237 The average $\text{PM}_{2.5}$ mass, OP_{AA} and OP_{DTT} data sets showed three different tendencies with respect to the
 238 locations. This is better visualised with their annual mean and median data in Fig. 1. The averages (i.e.
 239 the medians and means) of the $\text{PM}_{2.5}$ mass exhibited a rising trend with levelling off from the rural
 240 background through the suburban area to the city centre. The means of both $OP_{AA,m}$ and $OP_{AA,V}$ data sets
 241 indicated a maximum in the suburban background, whereas the tendencies for their medians were not
 242 fully conclusive. ~~The averages of both $OP_{DTT,m}$ and $OP_{DTT,V}$ data sets showed steadily increasing~~
 243 ~~behaviour.~~ The differences in the tendencies already suggest that there is a misalignment between the PM

244 mass and the OP data and that the two assays used show different sensitivity to source types active at the
 245 locations.

246

247

248

249

250

251

252

253

254

255

256

257

258

259

260

261

262

263

264

265

266

267

268

269

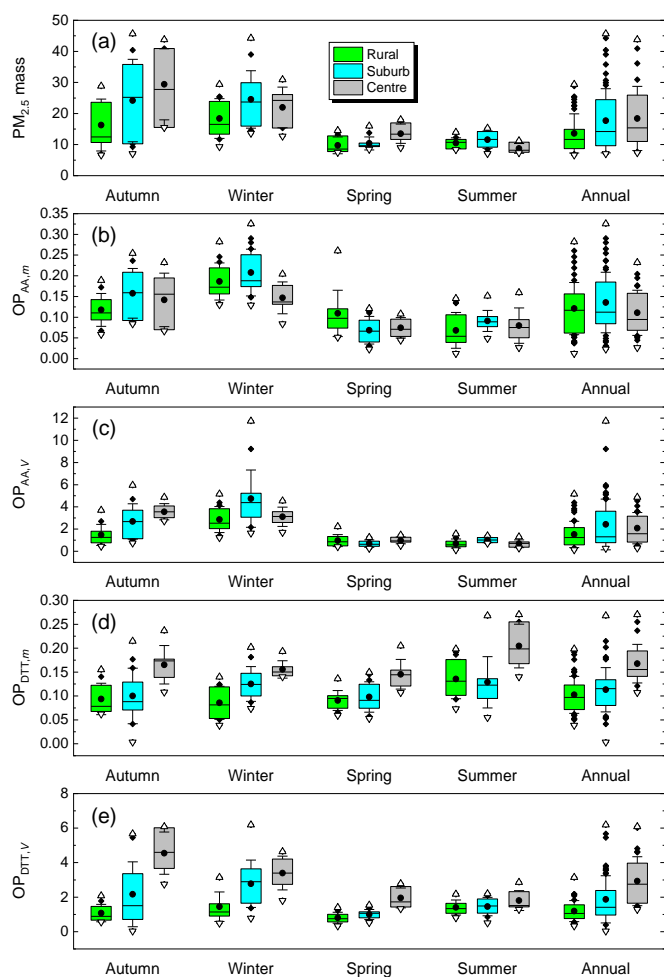
270

271

272

273

274



275 **Figure 1.** Box and whisker plots of PM_{2.5} mass concentration (μg m⁻³; panel a), oxidative potential (OP) determined by AA
 276 and DTT assays and normalised to PM mass (*m*; OP_{AA,*m*} and OP_{DTT,*m*}, nmol min⁻¹ μg⁻¹; panels b and d) or to sampled air
 277 volume (*V*; OP_{AA,*V*} and OP_{DTT,*V*}, nmol min⁻¹ m⁻³; panels c and e) in the rural background, suburban area and city centre
 278 separately for each season and over one year. Maximum and minimum values (triangles pointing upward and downward,
 279 respectively), further extreme values (diamonds), the first and third quartiles (lower and upper horizontal borders of the boxes,
 280 respectively), median (horizontal line inside the boxes), means (bullets) and ±1 SDs (whiskers) of the data sets are shown.

281

282 Basic statistics of PM_{2.5} mass and OP data separately for each season and the whole year are shown in
 283 Fig. 1. In winter and autumn (the heating period), the OP and PM mass levels were higher than in spring
 284 and summer. This is consistent with the other continental European sites (e.g. Calas et al., 2019; Borlaza
 285 et al., 2022). The heating period-to-non-heating period OP ratios in the urban locations were larger than
 286 for the rural background by factors of ca. 4 for OP_{AA,*V*} and 1–2 for OP_{DTT,*V*}. There were similar tendencies
 287 in the OP values derived by both AA and DTT assays over the seasons. Except for the OP_{DTT,*m*} data,

288 which showed a fairly constant level over the seasons with some higher values in summer, particularly in
289 the city centre. This can be again linked to the altered chemical composition of PM mass in time and to
290 the different responses of the two assays to this change.

291

292 There are only a few other OP data sets for the PM_{2.5} size fraction derived by AA and DTT assays. Their
293 comparison to our OP data is hindered by important experimental details such as the extracted amount of
294 PM from filters. It can be ~~roughly~~ identified that our median OP values are ~~somewhat~~ larger than those at
295 other European sites (Daellenbach et al., 2020; Grange et al., 2022, In 't Veld et al., 2023), while they
296 belong to the middle range of the available results for Japan and China (Kurihara et al., 2022; Yu et al.,
297 2019). The differences can be also influenced by the exact location type since higher OP data near traffic
298 sources were observed (Boogaard et al., 2012; Fang et al., 2016; Daellenbach et al., 2020).

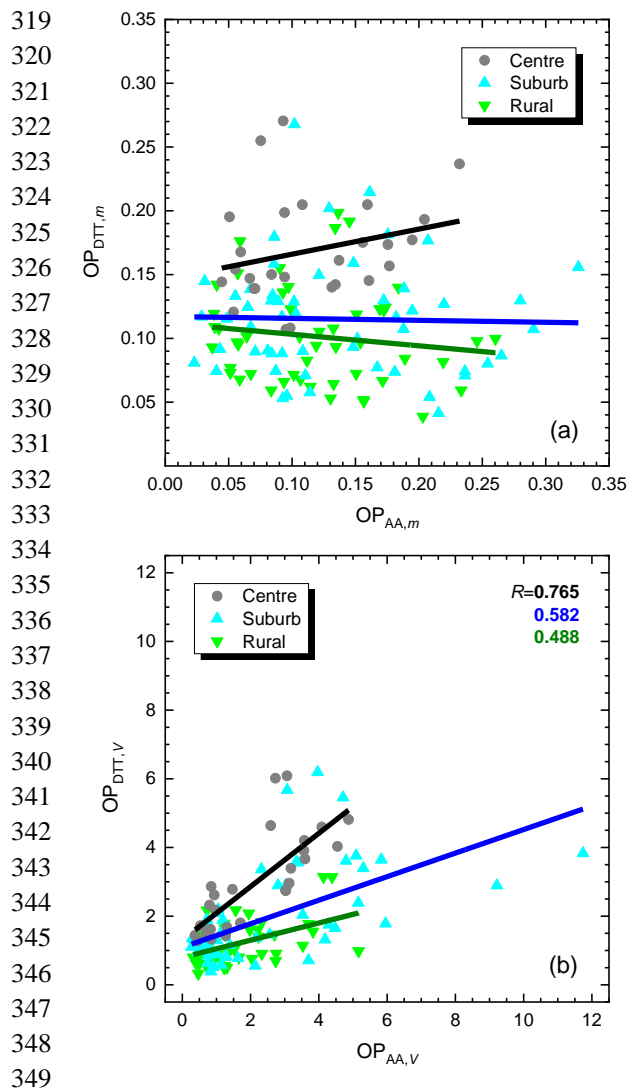
299 3.2 Consistency between the assays

300 The dependencies between the OP data derived by the AA assay and normalised either to m or V on the
301 corresponding DTT data are displayed in Fig. 2. Pearson's coefficients of correlation (R) between the data
302 sets normalised to m (Fig. 2a) were not significant ($p=0.05$) at the locations. It suggests that the OP_m was
303 controlled by chemical species that invoked different responses in the assays. However, all correlations
304 between the two OP data sets normalised to V (Fig. 2b) were significant. The slopes with SDs of the
305 regression lines were smaller than unity (0.25 ± 0.06 , 0.34 ± 0.07 and 0.78 ± 0.13 , respectively) and increased
306 monotonically from the rural background through the suburban area to the city centre.

307

308 The results suggested that the OP_{DTT} and OP_{AA} values normalised to sampled air volume were in line
309 and coherent consistent. The slopes of their regression lines (Fig. 2b) were <1 , which is interpreted as that
310 the AA assay reacted more sensitively to the changes in chemical composition of PM than the DTT
311 assay at our locations. ~~The increasing slope of the regression could be also connected to the fact that~~
312 organics of biogenic origin exhibit smaller responses in the DTT assays than those of BB (Verma et al.,
313 2015) or of urban sources in general. ~~The differences could be partly influenced by aerosol photochemical~~
314 aging and SOC formation over seasons (Wong et al., 2019; Zhang et al., 2022). More importantly, the
315 conclusions definitely underline the need for deploying multiple (at least two) OP assays, particularly in
316 cleaner atmospheric environments, to achieve a more wholistic and consistent picture (~~Bates et al., 2019;~~
317 Calas et al., 2017; Bates et al., 2019; Borlaza et al., 2022; Shahpoury et al., 2022).

318



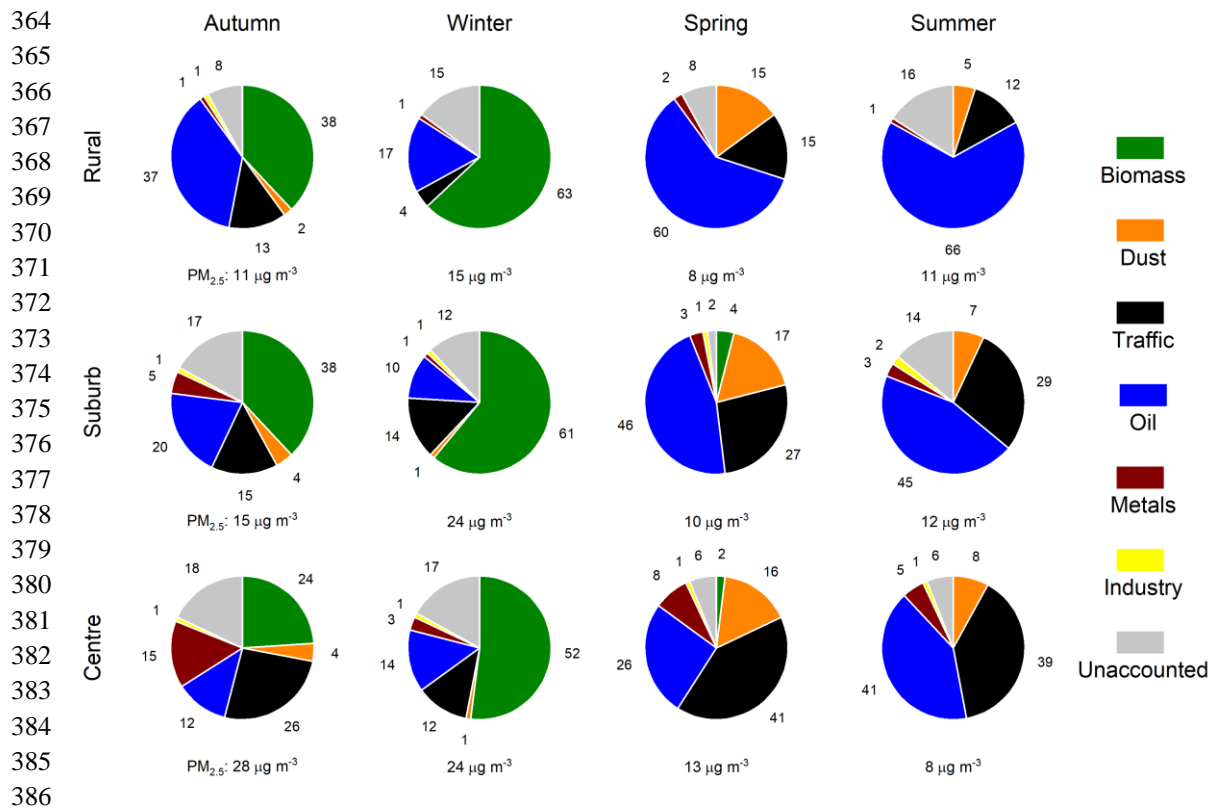
350 **Figure 2.** Scatter plots of the oxidative potential (OP) values determined by AA and DTT assays and normalised to PM mass
 351 (m ; $OP_{AA,m}$ and $OP_{DTT,m}$, in $\text{nmol min}^{-1} \mu\text{g}^{-1}$; panel a) or to sampled air volume (V ; $OP_{AA,V}$ and $OP_{DTT,V}$, $\text{nmol min}^{-1} \text{m}^{-3}$; panel
 352 b) separately in the rural background, suburban area and city centre. The coefficients of correlation (R s) for the significant
 353 cases are also given.

354 3.3 Main aerosol sources

355 Six factors resolved by the PMF modelling were further evaluated as described in Sect. S2. The following
 356 aerosol sources were identified: biomass burning, suspended dust, road traffic, oil combustion mixed with
 357 coal combustion and particularly, with long-range transport in the rural background during the nonheating
 358 period (Sect. S2), vehicle metal wear and mixed industrial source. Similar set of source types was also
 359 identified earlier for Budapest in larger number of samples in winter (Furu et al., 2022).

360

361 The apportionments of the $\text{PM}_{2.5}$ mass among the main sources are summarised in Fig. 3 separately for
 362 each location and season. The plots reveal that the source contributions changed very substantially over
 363 the year.



387 **Figure 3.** Mean contributions of biomass burning, suspended dust, road traffic, oil combustion mixed with coal combustion
 388 and long-range transport, vehicle metal wear, mixed industrial source and unaccounted sources to the atmospheric
 389 concentration of PM_{2.5} mass (in %) as derived by the PMF modelling in the rural background, suburban area and city centre in
 390 different seasons. The median atmospheric concentrations are shown under the circle charts.

391

392 In winter, BB was the dominant source (with mean contributions of 50 % – 60 %) at all sites. In autumn,
 393 BB and oil combustion (mixed with coal combustion and long-range transport) were the two most
 394 important sources in the rural background with similar shares (38 %). In the suburban area, BB exhibited
 395 very similar (38 %) contribution to the rural background, whereas oil combustion and the joint importance
 396 of road traffic and vehicle metal wear showed the second largest and similar contributions (20 %). In the
 397 city centre, traffic-related sources were the most important contributors (40 %). In spring, oil combustion
 398 prevailed (60 %) in the rural background. Its contribution monotonically decreased through the suburban
 399 area (46 %) to the city centre (26 %). In parallel with this tendency, the joint share from road traffic and
 400 vehicle metal wear increased monotonically (from 17 % through 30 % to 49 %) in the same order of the
 401 locations. The contributions from suspended dust in spring were also significant at all locations
 402 accounting for approximately 15%. They were influenced by the Saharan dust intrusion episodes
 403 extending over the whole Carpathian Basin in this season. In summer, oil combustion was again the
 404 dominant source (66 %) in the rural background and showed a decreasing share for the suburban area (45
 405 %) to the city centre (41 %). Contrary, the effects of road traffic monotonically rose (from 13 % through

406 31 % to 44 %). This increasing tendency was preserved in the other seasons as well. The unaccounted
407 sources and their possible effects on the final results are discussed in Sect. 3.6.

408

409 The apportionments of Cu and Fe, which are of special interest for OP, among the main aerosol sources
410 as derived by the PMF modelling are shown in Figs. S7 and S8. Copper mainly or dominantly originated
411 from motor vehicles, i.e. vehicle metal wear and road traffic sources except for the rural background in
412 winter and autumn. The outstanding role of road vehicles is confirmed by our earlier results for a street
413 canyon in central Budapest (Salma and Maenhaut, 2006). The smallest shares from vehicles occurred in
414 winter (22 %, 39 % and 65 %, respectively in the rural background, suburban area and city centre), while
415 the maximum contributions happened in summer (51 %, 65 % and 87 %, respectively). The contribution
416 of unaccounted sources in the rural background in winter was large (33 %), which could modify the
417 apportionments. The role of BB in Cu emissions could be possible explained by illegal industrial and
418 household waste burnings together with biomass (Sect. S2; Hoffer et al., 2021).

419

420 In the city centre, the vehicle sources showed the largest contributions to Fe (53 % – 74 %) in all seasons,
421 and dust was its second most intensive source (30 %–36 %) in spring and summer. At the other two
422 locations, Fe in spring was unambiguously dominated by dust (ca. 55 %), which was influenced by the
423 Saharan dust intrusion. Suspended dust remained the most important source in the rural background in
424 summer, whereas it became comparable to the traffic-related sources in the suburban area. Vehicles
425 tended to be the second largest Fe source (26 % – 45 %) in the rural background and suburban area. Their
426 contributions could be partly also associated with the resuspended road dust generated by moving
427 vehicles. In autumn, the shares in the rural background were more or less balanced among the main
428 sources, while the vehicle contributions were increased in the suburban area.

429

430 The examples of Cu and Fe demonstrated broadly varying spatial and temporal tendencies in the source
431 contributions of OP-active chemical species, and point to the potentials of regulatory measures based on
432 specifically selected source types.

433 **3.4 Oxidative potential and aerosol sources**

434 The OP data normalised to sampled air volume were apportioned to the main aerosol sources, i.e. of BB,
435 suspended dust, road traffic, oil combustion mixed with coal combustion and long-range transport, vehicle
436 metal wear and mixed industrial source using the MLR method with the WLS approach. The slopes and
437 intersect intercepts of the regression lines calculated for the whole data set at each sampling location are
438 summarised in Table S4. In a few cases, negative slopes were obtained. This is commonly found with this

439 approach, but the absolute values of the negative slopes should be relatively small. This was not the case
 440 for the vehicle metal wear and $OP_{DTT,V}$ pair in the rural background, for the road traffic and $OP_{AA,V}$ pair
 441 in the suburban area, and for the oil combustion and $OP_{AA,V}$ pair in the city centre. The ~~intersect~~ ~~intercepts~~
 442 of the $OP_{DTT,V}$ in the suburban area and city centre also resulted in statistically nonzero values. These
 443 cases jointly indicate that there could be some aerosol sources missing in the PMF modelling due probably
 444 to the unavailability of some important marker variables and to the limited number of samples. The
 445 shortcoming is further discussed in Sect. 3.6. It cannot be excluded that this imperfection influences the
 446 order and mainly the contributions of the OP sources. To improve the attribution of the OP to the identified
 447 aerosol sources, the MLR model with the WLS approach was also performed with forced positive slopes
 448 option. Its constrained results are summarised in Table 2.

449

450 **Table 2.** Slopes and ~~intersect~~ ~~intercepts~~ of the multiple linear regression with the weighted least squares approach and forced
 451 positive slopes option between oxidative potential (OP) determined by AA and DTT assays and normalised to sampled air
 452 volume ($OP_{AA,V}$ and $OP_{DTT,V}$, respectively; in $nmol\ min^{-1}\ m^{-3}$) and the main aerosol sources of biomass burning, suspended
 453 dust, road traffic, oil combustion ~~mixed with coal combustion and long-range transport~~, vehicle metal wear and mixed
 454 industrial source derived by PMF modelling in the rural background, suburban area and city centre. The number of samples
 455 available (n) and the adjusted coefficients of determination (R^2) are also shown. Nonsignificant values are in *Italic* font.

456

Location/ Main source	Rural background		Suburban area		City centre	
	$OP_{AA,V}$	$OP_{DTT,V}$	$OP_{AA,V}$	$OP_{DTT,V}$	$OP_{AA,V}$	$OP_{DTT,V}$
Biomass burning	1.414	0.873	0.792	0.622	1.073	0.788
Suspended dust	<i>0.113</i>	–	0.569	<i>0.018</i>	<i>0.025</i>	<i>0.090</i>
Road traffic	1.010	0.959	–	<i>0.181</i>	0.357	0.887
Oil combustion	0.279	–	<i>0.522</i>	0.968	–	<i>0.488</i>
Vehicle metal wear	<i>0.056</i>	–	–	–	<i>0.018</i>	<i>0.091</i>
Mixed industrial	–	<i>0.085</i>	<i>0.172</i>	<i>0.086</i>	<i>0.142</i>	–
Intersect Intercept	<i>-0.160</i>	<i>0.358</i>	<i>-0.473</i>	<i>-0.497</i>	<i>-0.081</i>	<i>-0.362</i>
n	52	51	56	55	28	28
R^2	0.974	0.877	0.717	0.779	0.858	0.811

457

458 With this latter option, all ~~intersect~~ ~~intercepts~~ became statistically insignificant ($p < 0.05$) from zero. The
 459 AA assay yielded significant slopes with BB, road traffic and oil combustion in the rural background,
 460 with BB and suspended dust in the suburban area and with BB, and road traffic in the city centre. The
 461 DTT assay resulted in significant slopes with BB and road traffic, with BB and oil combustions and with
 462 BB and road traffic in the three environments. Comparing the fitted MLR parameters obtained by the
 463 constrained and non-constrained WLS approaches (Tables 2 and S4) shows that the orders of the sources
 464 did not change substantially, and that the positive slopes obtained by the two models are comparable. At

465 the same time, the importance of oil combustion decreased in some occasions. These likely indicate that
466 the derived ranks of the OP sources are sensible approximations to reality with some larger uncertainties
467 of their contributions.

468

469 The driving effect of BB on OP has been highlighted in other studies (e.g. Verma et al., 2015; Lionetto et
470 al., 2021; Borlaza et al., 2022). The intensity of BB in the Carpathian Basin is, however, large only in the
471 heating period (autumn and winter), and much lower outside this interval. To refine the apportionment of
472 the OP data to aerosol sources active in the non-heating seasons, the MLR modelling was repeated with
473 the joint data set of all sites split into heating and non-heating periods. These results confirmed that BB
474 shows overwhelming contributions to the OP values in the heating period independently of the intensity
475 of the vehicle road traffic. The latter changed substantially among the rural background and urban sites.
476 More importantly, the obtained results also imply that the shares from vehicles (i.e. joint sources of road
477 traffic and vehicle metal wear) to OP prevailed in the non-heating period. This is in line with the
478 attributions of some transition metals such as Cu and Fe to these aerosol sources (Figs. S7–S8 and Salma
479 and Maenhaut, 2006), and also points to the remarkable role of primary traffic emissions in causing
480 oxidative stress in spring and summer.

481

482 Secondary organic aerosol under anthropogenically influenced conditions was proven to be one of the top
483 factors for OP (Srivastava et al., 2018; Wong et al., 2019; Daellenbach et al., 2020; Borlaza et al., 2021a,
484 2021b; Pye et al., 2021; Zhang et al., 2022). The involvement of the SOC concentrations into the PMF
485 was hampered by their smaller count and larger relative uncertainty (up to 30 % – 50 %; Salma et al.,
486 2022). Instead, we investigated the correlations between the OP data sets and SOC concentrations or
487 SOC/OC ratios. The dependencies of the $OP_{DTT,V}$ on the SOC are shown in Fig. S9. The OP values at the
488 urban locations tended to increase with the SOC in parallel with each other, while the OP was rising in a
489 smaller rate in the regional background. The reasons behind these observations likely include the distinct
490 effects of biogenic and anthropogenic secondary organic aerosols typically present in different portions
491 at the sampling locations. The results may ~~also~~ indirectly indicate that photochemical aging processes and
492 SOC formation over seasons impact the ~~toxicity-OP~~ of PM as well (Wong et al., 2019; Kodros et al.,
493 2020; Zhang et al., 2022). The increasing slope of the regression lines from the rural background to the
494 city centre shown in Fig. 2b may also imply that organics of biogenic origin exhibit smaller responses in
495 the DTT assays than those of BB (Verma et al., 2015) or of urban sources in general. There were no
496 significant correlations obtained for the other data pairs.

497 3.5 Oxidative potential and air quality

498 Particulate matter mass was proven to be the most important ~~proximity metric~~ component from the criteria
499 air pollutants ~~for the general air quality~~ in the Carpathian Basin (Salma et al., 2020a, 2020b). Generally,
500 this measure expresses the air quality in the basin. Therefore, the relationships between the PM_{2.5} mass
501 and OP data sets normalised to sampled air volume were separately investigated. Their correlation
502 dependencies were all significant (Fig. 4). Spatial and temporal correlations between these variables from
503 low to moderate were also observed in earlier studies under broadly varying conditions (Künzli et al.,
504 2006; Boogaard et al., 2012; Yang et al., 2015; Fang et al., 2016; Chirizzi et al., 2017).

505

506

507

508

509

510

511

512

513

514

515

516

517

518

519

520

521

522

523

524

525

526

527

528

529

530

531

532

533

534

535

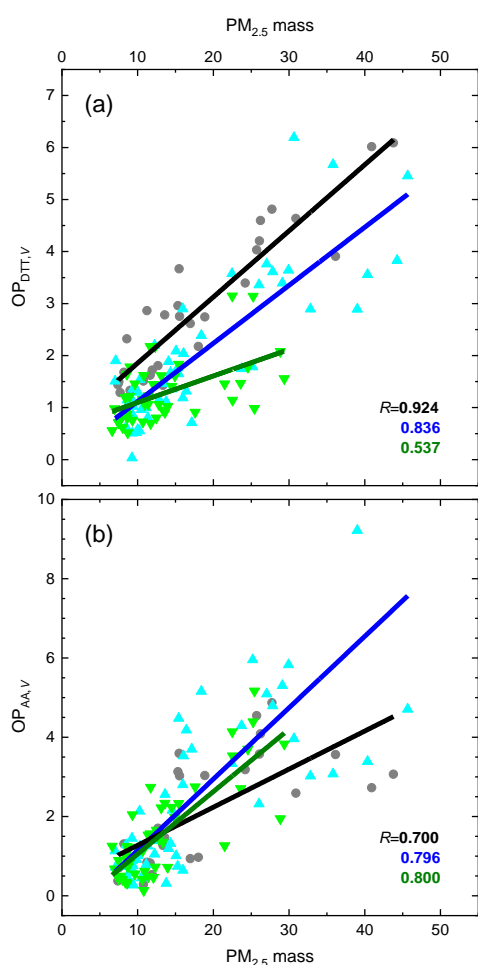
536

537

538

539

540



534 **Figure 4.** Scatter plots of the oxidative potential (OP) determined by DTT (a) and AA (b) assays and normalised to sampled
535 air volume (*V*; OP_{DTT,*V*} and OP_{AA,*V*}, respectively, in nmol min⁻¹ m⁻³) and PM_{2.5} mass concentrations (µg m⁻³) for the rural
536 background, suburban area and city centre. The lines represent linear regressions of the data sets. The coefficients of correlation
537 (*R*s) are also indicated.

538

539 The dependencies for the OP_{DTT,*V*} (Fig. 4a) resulted in two almost parallel lines (with slopes and SDs of
540 0.11±0.01 and 0.13±0.01 nmol min⁻¹ µg⁻¹, respectively) in the city centre and suburban area, while a

541 smaller slope ($0.051 \pm 0.012 \text{ nmol min}^{-1} \mu\text{g}^{-1}$) was observed in the rural background. The situation for the
542 $\text{OP}_{\text{AA,V}}$ (Fig. 4b) was less obvious but somewhat similar to $\text{OP}_{\text{DTT,V}}$. The regression lines for the rural
543 background and suburban area tended to be fairly parallel with each other (with slopes and SDs of
544 0.16 ± 0.02 and $0.18 \pm 0.02 \text{ nmol min}^{-1} \mu\text{g}^{-1}$, respectively), whereas the slope for the city centre was smaller
545 ($0.096 \pm 0.019 \text{ nmol min}^{-1} \mu\text{g}^{-1}$). The ~~interseet~~ intercepts could be typically regarded to be zero within the
546 uncertainty interval.

547

548 The parallel tendencies may indicate that the effects of the PM chemical compositions on the given assay
549 were close to each other at the sampling locations with the parallel lines. This was likely caused by spatial
550 and temporal similarities in the main sources such as road traffic and resuspended dust particularly for
551 the DTT assay, and biomass burning especially for the AA assay (Salma et al., 2020a). Particles in the
552 third environment (with the smaller slope) likely contained less OP-active components from the point of
553 the given assay and, therefore, the increase in the OP was more modest. This interpretation is confirmed
554 by earlier similar conclusions (Daellenbach et al., 2020). Nevertheless, it should be stressed that all slopes
555 were substantially and much smaller than unity. This implies that the air quality regulatory measures
556 based on the $\text{PM}_{2.5}$ mass are expected to result in smaller improvements in oxidative stress compared to
557 dedicated measures that specifically target (appropriately selected) aerosol sources.

558 **3.6 Limitations and later possibilities**

559 The total numbers of the samples collected at each location represent a limitation mainly for the PMF
560 modelling. To overcome this problem, we applied multisite PMF. It was implicitly assumed in this
561 approach that the main sources active at the locations can be characterised by similar chemical profiles.
562 This is not completely fulfilled for all seasons. An example is the suspended dust which is virtually
563 fugitive mineral and soil dust made of geogenic elements in the rural backgrounds. In the urban sites, it
564 contains further constituents originally generated by anthropogenic activities, which settled down to
565 surfaces and later entered into the air again by resuspension. It is mentioned that the PMF modelling on
566 the separate locations yielded fairly similar results to the multisite approach, while the statistical
567 uncertainties of these latter calculations were favourable.

568

569 The unavailability of some secondary inorganics, mainly nitrate and ammonium ions in the present
570 analytical data sets introduced another limitation. Their contributions were likely contained in the
571 unaccounted sources of the PMF modelling. They ranged up to 18 % and showed contributions mainly in
572 colder (heating) seasons or in summer for the rural background and suburban area. Fortunately, pure
573 secondary inorganic constituents are associated with lower contribution to OP of PM-toxicity (Cassee et

574 al., 2013; Daellenbach et al., 2020), although they can influence the OP through acid mediated dissolution
575 of transition metals (Fang et al., 2017). However, the robustness of the PMF modelling can influence the
576 final apportion of the OP among the resolved sources.

577

578 Larger number of samples and extended list of variables are ~~pronouncedly~~ required because of the basin
579 character of the region of interest. The poorest air quality in the whole Carpathian Basin generally occurs
580 in winter (Salma et al., 2022), when persistent anticyclonic weather situations and lasting temperature
581 inversions happen for longer times. During these intervals, the time series of aerosol constituents, even
582 of different origins, change coherently at many locations due to the common effects of regional
583 meteorology. This dependency can further encumber the separation of the aerosol sources in PMF
584 modelling (Salma et al., 2004).

585

586 The present results and conclusions for the OP are strictly valid for the concrete sample preparation and
587 selected assays. A more holistic picture can be achieved by deploying additional and extended
588 experimental methods including those for the sample extraction treatment and OP measurement
589 comprising advantageously both cellular and possibly further acellular assays. The present outcomes can
590 be ~~further~~ also improved by involving additional important chemical species and markers, mainly water-
591 soluble metal ions, water-soluble OC, primary biogenic OC and PAHs. Extended research is required to
592 address some additional relevant sources such as coal combustion, biogenic emissions and illegal waste
593 burning. Investigations of size-fractionated aerosol samples with several toxicity indicators ~~including~~
594 ~~intra~~ cellular tests and possible synergism or antagonism among chemical species could bring further
595 insights into the oxidative stress research. The experience gained in the present work, which was
596 conducted in a systematic manner for the first time in this region, can form valuable experience in
597 planning further related studies.

598 **4 Conclusions**

599 We showed that the OP induced by PM_{2.5} mass and determined by the AA and DTT assays in the rural
600 (regional) background of the Carpathian Basin, in the suburban area and centre of its largest city of
601 Budapest differed substantially and in a complex manner with location and changed considerably and
602 consistently with season. The alterations were mainly caused by varying intensities of the main aerosol
603 sources and possibly by other specific seasonal features. Biomass burning clearly exhibited the dominant
604 influence at all locations in the heating period. Several pieces of indirect evidence suggest that the joint

605 effects of motor vehicles involving road traffic and vehicle metal wear played the most important role in
606 summer and spring, with considerable contributions from oil combustion and resuspended dust.

607

608 The most severe daily PM health limit exceedances in Budapest (and several other European cities) occur
609 in winter due to both residential heating and meteorological effects. The contributions of BB to OP are
610 the largest during this season. Thus, human exposure to high pollution levels are further exacerbated by
611 the chemical composition which causes increased oxidative stress. As far as the sources related to motor
612 vehicles are concerned, large traffic intensities frequently occur in city centres, which generate dangerous
613 hotspots of particularly OP-active species. In these sites, an enhanced exposure of public in summer and
614 spring often coincides with high population densities.

615

616 Our conclusions imply that targeting the PM mass in general does not efficiently reduce the oxidative
617 burden from PM exposure. Instead, substantial health improvements could be achieved by focusing on
618 some specific source types such as BB in winter and vehicle traffic in non-heating period. The former
619 source may have timely consequences since it is expected to be increased in the near future. The non-
620 exhaust emissions from vehicle traffic are anticipated to gain in relevance as well since high-efficiency
621 exhaust gas aftertreatment devices had been already adopted to internal combustion engines and because
622 of global spreading of electric vehicles. The advantages of BB and electric cars are often emphasized,
623 while their potential drawbacks have been less disseminated. It is needed to further investigate their
624 distinctive health effects for setting up effective mitigation policies and season-specific regulations.

625 *Data availability.* The observational data are available from the corresponding author.

626 *Supplement.* The supplement related to this article is available online at: *to be completed.*

627 *Author contributions.* MV evaluated the data, performed the modelling calculations, prepared figures, participated in
628 interpreting the results and contributed to writing the manuscript; GU and J-LJ managed the OP measurements, GU, J-LJ and
629 PD participated in interpreting the results and revising the manuscript; ZsK and EP managed the PIXE measurements and
630 participated in interpreting the PMF results; IS conceived the research, arranged the sample collections, evaluated and
631 interpreted the results, prepared figures, wrote the manuscript. All coauthors reviewed and commented on the manuscript.

632 *Competing interests.* The authors declare that they have no conflict of interest.

633 *Acknowledgements.* The authors are grateful to Anikó Angyal of the Institute for Nuclear Research for the PIXE measurements,
634 to Attila Machon of the Hungarian Meteorological Service for the assistance in the sample collections and the OC/EC
635 measurements, and to Anikó Vasanits of the Eötvös Loránd University for the LVG measurements.

636 *Financial support.* This research has been supported by the Hungarian Research, Development and Innovation Office (grants
637 K132254 and K146915), the European Regional Development Fund and the Hungarian Government (grant GINOP-2.3.3-15-
638 2016-00005) and the New National Excellence Program of the Ministry for Innovation and Technology from the source of the
639 Hungarian Research, Development and Innovation Fund (ÚNKP-21-3). The OP analysis was supported by the ACME program
640 (ANR-15-IDEX-02) and ANR Get OP Stand OP program (ANR-19-CE34-0002-01), and were analysed at the Air-O-Sol
641 facility at IGE, made possible with the funding of some laboratory equipment by the Labex OSUG@2020 (ANR10 LABX56).

642 **References**

- 643 Abrams, J. Y., Weber, R. J., Klein, M., Samat, S. E., Chang, H. H., Strickland, M. J., Verma, V., Fang, T., Bates, J. T.,
644 Mulholland, J. A., Russell, A. G., and Tolbert, P. E.: Associations between ambient fine particulate oxidative potential
645 and cardiorespiratory emergency department visits, *Environ. Health Perspect.*, 125, 107008,
646 <https://doi.org/10.1289/EHP1545>, 2017.
- 647 Aljboor, S., Angyal, A., Baranyai, D., Kertész, Zs., Papp, E., Szarka, M., Szikszai, Z., Rajta, I., and Vajda, I.: Light element
648 sensitive in-air millibeam-PIXE setup for fast measurement of atmospheric aerosol samples, *J. Anal. At. Spectrom.*,
649 submitted in 2022.
- 650 Apte, J. S., Marshall, J. D., Cohen, A. J., and Brauer, M.: Addressing global mortality from ambient PM_{2.5}, *Environ. Sci.*
651 *Technol.*, 49, 8057–8066, <https://doi.org/10.1021/acs.est.5b01236>, 2015.
- 652 Ayres, J. G., Borm, P., Cassee, F. R., Castranova, V., Donaldson, K., Ghio, A., Harrison, R. M., Hider, R., Kelly, F., Kooter,
653 I. M., Marano, F., Maynard, R. L., Mudway, I., Nel, A., Sioutas, C., Smith, S., Baeza-Squiban, A., Cho, A., Duggan, S.,
654 and Froines, J.: Evaluating the toxicity of airborne particulate matter and nanoparticles by measuring oxidative stress
655 potential— a workshop report and consensus statement, *Inhal. Toxicol.* 20, 75–99,
656 <https://doi.org/10.1080/08958370701665517>, 2008.
- 657 Baumann, K., Wietzoreck, M., Shahpoury, P., Filippi, A., Hildmann, S., Lelieveld, S., Berkemeier, T., Tong, H., and
658 Lammel, G.: Is the oxidative potential of components of fine particulate matter surface-mediated?, *Environ. Sci. Pollut.*
659 *Res.*, 30, 16749–16755, <https://doi.org/10.1007/s11356-022-24897-3>, 2023.
- 660 Bates, J. T., Weber, R. J., Abrams, J., Verma, V., Fang, T., Klein, M., Strickland, M. J., Sarnat, S. E., Chang, H. H.,
661 Mulholland, J. A., Tolbert, P. E., and Russell, A. G.: Reactive oxygen species generation linked to sources of
662 atmospheric particulate matter and cardiorespiratory effects, *Environ. Sci. Technol.*, 49, 13605–13612,
663 <https://doi.org/10.1021/acs.est.5b02967>, 2015.
- 664 Bates, J. T., Fang, T., Verma, V., Zeng, L., Weber, R. J., Tolbert, P. E., Abrams, J. Y., Sarnat, S. E., Klein, M., Mulholland,
665 J. A., and Russell, A. G.: Review of acellular assays of ambient particulate matter oxidative potential: methods and
666 relationships with composition, sources, and health effects, *Environ. Sci. Technol.*, 53, 4003–4019,
667 <https://doi.org/10.1021/acs.est.8b03430>, 2019.
- 668 Blumberger, Z. I., Vasanits-Zsigrai, A., Farkas, G., and Salma, I.: Mass size distribution of major monosaccharide
669 anhydrides and mass contribution of biomass burning, <https://doi.org/10.1016/j.atmosres.2019.01.001>, *Atmos. Res.*,
670 220, 1–9, 2019.
- 671 Boogaard, H., Janssen, N. A. H., Fischer, P. H., Kos, G. P. A., Weijers, E. P., Cassee, F. R., van der Zee, S. C., de Hartog, J.
672 J., Brunekreef, B., and Hoek G.: Contrasts in oxidative potential and other particulate matter characteristics collected
673 near major streets and background locations, *Environ. Health Perspect.*, 120, 2, <https://doi.org/10.1289/ehp.1103667>,
674 2012.
- 675 Bondy, S. C.: Anthropogenic pollutants may increase the incidence of neurodegenerative disease in an aging population,
676 *Toxicology*, 341–343, 41–46, <https://doi.org/10.1016/j.tox.2016.01.007>, 2016.
- 677 Borlaza, L. J. S., Weber, S., Uzu, G., Jacob, V., Cañete, T., Micallef, S., Trébuchon, C., Slama, R., Favez, O., and Jaffrezo,
678 J.-L.: Disparities in particulate matter (PM₁₀) origins and oxidative potential at a city scale (Grenoble, France) – Part 1:
679 Source apportionment at three neighbouring sites, *Atmos. Chem. Phys.*, 21, 5415–5437, [https://doi.org/10.5194/acp-21-](https://doi.org/10.5194/acp-21-5415-2021)
680 5415-2021, 2021a.
- 681 Borlaza, L. J. S., Weber, S., Jaffrezo, J.-L., Houdier, S., Slama, R., Rieux, C., Albinet, A., Micallef, S., Trébluchon, C., and
682 Uzu, G.: Disparities in particulate matter (PM₁₀) origins and oxidative potential at a city scale (Grenoble, France) – Part
683 2: Sources of PM₁₀ oxidative potential using multiple linear regression analysis and the predictive applicability of
684 multilayer perceptron neural network analysis, *Atmos. Chem. Phys.*, 21, 9719–9739, [https://doi.org/10.5194/acp-21-](https://doi.org/10.5194/acp-21-9719-2021)
685 9719-2021, 2021b.
- 686 Borlaza, L. J., Weber, S., Marsal, A., Uzu, G., Jacob, V., Besombes, J.-L., Chatain, M., Conil, S., and Jaffrezo, J.-L.: Nine-
687 year trends of PM₁₀ sources and oxidative potential in a rural background site in France, *Atmos. Chem. Phys.*, 22,
688 8701–8723, <https://doi.org/10.5194/acp-22-8701-2022>, 2022.
- 689 Borm, P. J. A., Kelly, F., Künzli, N., Schins, R. P. F., and Donaldson, K.: Oxidant generation by particulate matter: from
690 biologically effective dose to a promising, novel metric, *Occup. Environ. Med.*, 64, 73–74,
691 <https://doi.org/10.1136/oem.2006.029090>, 2007.
- 692 Calas, A., Uzu, G., Martins, J. M. F., Voisin, D., Spadini, L., Lacroix, T., and Jaffrezo, J.-L.: The importance of simulated
693 lung fluid (SLF) extractions for a more relevant evaluation of the oxidative potential of particulate matter, *Sci. Rep.* 7,
694 11617, <https://doi.org/10.1038/s41598-017-11979-3>, 2017.

695 Calas, A., Uzu, G., Kelly, F. J., Houdier, S., Martins, J. M. F., Thomas, F., Molton, F., Charron, A., Dunster, C., Oliete, A.,
696 Jacob, V., Besombes, J.-L., Chevrier, F., and Jaffrezo, J.-L.: Comparison between five acellular oxidative potential
697 measurement assays performed with detailed chemistry on PM₁₀ samples from the city of Chamonix (France), *Atmos.*
698 *Chem. Phys.*, 18, 7863–7875, <https://doi.org/10.5194/acp-18-7863-2018>, 2018.

699 Calas, A., Uzu, G., Besombes, J.-L., Martins, J. M. F., Redaelli, M., Weber, S., Charron, A., Albinet, A., Chevrier, F.,
700 Brulfert, G., Mesbah, B., Favez, O., and Jaffrezo, J.-L.: Seasonal variations and chemical predictors of oxidative
701 potential (OP) of particulate matter (PM), for seven urban French sites, *Atmosphere*, 10, 698,
702 <https://doi.org/10.3390/atmos10110698>, 2019.

703 Cassee, F. R., Héroux, M.-E., Gerlofs-Nijland, M. E., and Kelly, F. J.: Particulate matter beyond mass: recent health
704 evidence on the role of fractions, chemical constituents and sources of emission, *Inhal. Toxicol.*, 25, 802–812,
705 <https://doi.org/10.3109/08958378.2013.850127>, 2013.

706 Cavalli, F., Viana, M., Yttri, K. E., Genberg, J., and Putaud, J.-P.: Toward a standardised thermal-optical protocol for
707 measuring atmospheric organic and elemental carbon: the EUSAAR protocol, *Atmos. Meas. Tech.*, 3, 79–89,
708 <https://doi.org/10.5194/amt-3-79-2010>, 2010.

709 Charrier, J. G. and Anastasio, C.: On dithiothreitol (DTT) as a measure of oxidative potential for ambient particles: evidence
710 for the importance of soluble transition metals, *Atmos. Chem. Phys.*, 12, 9321–9333, <https://doi.org/10.5194/acp-12-9321-2012>, 2012.

712 Charrier, J. G., McFall, A. S., Vu, K. K.-T., Baroi, J., Olea, C., Hasson, A., and Anastasio, C.: A Bias in the “Mass-
713 Normalized” DTT Response – An Effect of Non-Linear Concentration-Response Curves for Copper and Manganese,
714 *Atmos. Environ.*, 144, 325–334, <https://doi.org/10.1016/j.atmosenv.2016.08.071>, 2016.

715 Chiari, M., Yubero, E., Calzolari, G., Lucarelli, F., Crespo, J., Galindo, N., Nicolás, J. F., Giannoni, M., and Nava, S.:
716 Comparison of PIXE and XRF analysis of airborne particulate matter samples collected on Teflon and quartz fibre
717 filters, *Nucl. Instrum. Meth. B*, 417, 128–132, <https://doi.org/10.1016/j.nimb.2017.07.031>, 2018.

718 Chirizzi, D., Cesari, D., Guascito, M. R., Dinoi, A., Giotta, L., Donateo, A., and Contini, D.: Influence of Saharan dust
719 outbreaks and carbon content on oxidative potential of water-soluble fractions of PM_{2.5} and PM₁₀, *Atmos. Environ.*,
720 163, 1–8, <https://doi.org/10.1016/j.atmosenv.2017.05.021>, 2017.

721 Cho, A. K., Sioutas, C., Miguel, A. H., Kumagai, Y., Schmitz, D. A., Singh, M., Eiguren-Fernandez, A., and Froines, J. R.:
722 Redox activity of airborne particulate matter at different sites in the Los Angeles Basin, *Environ. Res.*, 99, 40–47,
723 <https://doi.org/10.1016/j.envres.2005.01.003>, 2005.

724 Cohen, A., Brauer, M., Burnett, R., Anderson, H., Frostad, J., Estep, K., Balakrishnan, K., Brunekreef, B., Dandona, L.,
725 Dandona, R., Feigin, V., Freedman, G., Hubbell, B., Jobling, A., Kan, H., Knibbs, L., Liu, Y., Martin, R., Morawska,
726 L., and Forouzanfar, M.: Estimates and 25-year trends of the global burden of disease attributable to ambient air
727 pollution: An analysis of data from the Global Burden of Diseases Study 2015, *The Lancet*, 389, 1907–1918,
728 [https://doi.org/10.1016/S0140-6736\(17\)30505-6](https://doi.org/10.1016/S0140-6736(17)30505-6), 2017.

729 Daellenbach, K. R., Uzu, G., Jiang, J., Cassagnes, L.-E., Leni, Z., Vlachou, A., Stefanelli, G., Canonaco, F., Weber, S.,
730 Segers, A., Kuenen, J. J. P., Schaap, M., Favez, O., Albinet, A., Aksoyoglu, S., Dommen, J., Baltensperger, U., Geiser,
731 M., El Haddad, I., Jaffrezo, J.-L., and Prévôt, A. S. H.: Sources of particulate-matter air pollution and its oxidative
732 potential in Europe, *Nature*, 587, 414–419, <https://doi.org/10.1038/s41586-020-2902-8>, 2020.

733 Dhalla, N., Temsah, R. M., and Netticadan, Th.: Role of oxidative stress in cardiovascular diseases, *J. Hypertens.*, 18,
734 [https://doi.org/655–673](https://doi.org/655-673), 10.1097/00004872-200018060-00002, 2000.

735 Dai, Q., Hopke, Ph. K., Bi, X., and Feng, Y.: Improving apportionment of PM_{2.5} using multisite PMF by constraining G-
736 values with a priori information, *Sci. Total Environ.*, 736, 139657, <https://doi.org/10.1016/j.scitotenv.2020.139657>,
737 2020.

738 Donaldson, K., Tran, L., Jimenez, L., Duffin, R., Newby, D., Mills, N., MacNee, W., and Stone, V.: Combustion-derived
739 nanoparticles: a review of their toxicology following inhalation exposure, *Part. Fibre Toxicol.*, 2, 10,
740 <https://doi.org/10.1186/1743-8977-2-10>, 2005.

741 EPA: Positive matrix factorization model for environmental data analyses, [https://www.epa.gov/air-research/positive-](https://www.epa.gov/air-research/positive-matrix-factorization-model-environmental-data-analyses)
742 [matrix-factorization-model-environmental-data-analyses](https://www.epa.gov/air-research/positive-matrix-factorization-model-environmental-data-analyses), last access: 20 June 2022, 2017.

743 Fang, T., Verma, V., Bates, J. T., Abrams, J., Klein, M., Strickland, M. J., Sarnat, S. E., Chang, H. H., Mulholland, J. A.,
744 Tolbert, P. E., Russell, A. G., and Weber, R. J.: Oxidative potential of ambient water-soluble PM_{2.5} in the southeastern
745 United States: contrasts in sources and health associations between ascorbic acid (AA) and dithiothreitol (DTT) assays,
746 *Atmos. Chem. Phys.*, 16, 3865–3879, <https://doi.org/10.5194/acp-16-3865-2016>, 2016.

747 Fang, T., Guo, H., Zeng, L., Verma, V., Nenes, A., and Weber, R. J.: Highly acidic ambient particles, soluble metals, and
748 oxidative potential: a link between sulfate and aerosol toxicity, *Environ. Sci. Technol.*, 51, 2611–2620,
749 <https://doi.org/10.1021/acs.est.6b06151>, 2017.

750 Furu, E., Angyal, A., Szoboszlai, Z., Papp, E., Török, Z., and Kertész, Z.: Characterization of aerosol pollution in two
751 Hungarian cities in winter 2009–2010, *Atmosphere*, 13, 554, <https://doi.org/10.3390/atmos13040554>, 2022.

752 Gao, D., Ripley, S., Weichenthal, S., and Godri Pollitt, K. J.: Ambient particulate matter oxidative potential: chemical
753 determinants, associated health effects, and strategies for risk management, *Free Radic. Biol. Med.*, 151, 7–25,
754 <https://doi.org/10.1016/j.freeradbiomed.2020.04.028>, 2020.

755 Godri, K. J., Harrison, R. M., Evans, T., Baker, T., Dunster, C., Mudway, I. S., and Kelly, F. J.: Increased oxidative burden
756 associated with traffic component of ambient particulate matter at roadside and urban background schools sites in
757 London, *PLoS One*, 6, 1–11, <https://doi.org/10.1371/journal.pone.0021961>, 2011.

758 Grange, S. K., Uzu, G., Weber, S., Jaffrezo, J.-L., and Hueglin, C.: Linking Switzerland's PM₁₀ and PM_{2.5} oxidative potential
759 (OP) with emission sources, *Atmos. Chem. Phys.*, 22, 7029–7050, <https://doi.org/10.5194/acp-22-7029-2022>, 2022.

760 Hoffer, A., Tóth, Á., Jancsek-Turóczi, B., Machon, A., Meiramova, A., Nagy, A., Marmureanu, L., and Gelencsér, A.:
761 Potential new tracers and their mass fraction in the emitted PM₁₀ from the burning of household waste in stoves,
762 *Atmos. Chem. Phys.*, 21, 17855–17864, <https://doi.org/10.5194/acp-21-17855-2021>, 2021.

763 Hopke, P. K.: Review of receptor modeling methods for source apportionment, *J. Air. Waste Manag. Assoc.*, 66, 237–259,
764 <https://doi.org/10.1080/10962247.2016.1140693>, 2016.

765 Hopke, P. K.: A guide to positive matrix factorization, Clarkson University, Potsdam, USA, 2000.

766 In 't Veld, M., Pandolfi, M., Amato, F., Pérez, N., Reche, C., Dominutti, P., Jaffrezo, J.-L., Alastuey, A., Querol, X., and
767 Uzu, G.: Discovering oxidative potential (OP) drivers of atmospheric PM₁₀, PM_{2.5}, and PM₁ simultaneously in North-
768 Eastern Spain, *Sci. Total Environ.*, 857, 159386, <https://doi.org/10.1016/j.scitotenv.2022.159386>, 2023.

769 [Janssen, N. A. H., Yang, A., Strak, M., Steenhof, M., Hellack, B., Gerlofs-Nijland, M. E., Kuhlbusch, T., Kelly, F., Harrison,
770 R., Brunekreef, B., Hoek, G., and Cassee, F.: Oxidative potential of particulate matter collected at sites with different
771 source characteristics, *Sci. Total Environ.*, 472, 572–581, <https://doi.org/10.1016/j.scitotenv.2013.11.099>, 2014.](https://doi.org/10.1016/j.scitotenv.2013.11.099)

772 Katerji, M., Filippova, M., and Duerksen-Hughes, P.: Approaches and methods to measure oxidative stress in clinical
773 samples: research applications in the cancer field, *Oxidative Med. Cell. Longev.*, 12, 1279250,
774 <https://doi.org/10.1155/2019/1279250>, 2019.

775 Kelly, F. J. and Mudway, I. S.: Protein oxidation at the air-lung interface, *Amino Acids*, 25, 375–396,
776 <https://doi.org/10.1007/s00726-003-0024-x>, 2003.

777 Kelly, F. J. and Fussell, J. C.: Size, source and chemical composition as determinants of toxicity attributable to ambient
778 particulate matter, *Atmos. Environ.*, 60, 504–526, <https://doi.org/10.1016/j.atmosenv.2012.06.039>, 2012.

779 Kelly, F. J. and Fussell, J. C.: Air pollution and public health: emerging hazards and improved understanding of risk,
780 *Environ. Geochem. Health*, 37, 631–649, <https://doi.org/10.1007/s10653-015-9720-1>, 2015.

781 Kelly, F. J. and Fussell, J. C.: Toxicity of airborne particles-established evidence, knowledge gaps and emerging areas of
782 importance, *Philos. Trans. R. Soc.*, A378, 2019.0322, <https://doi.org/10.1098/rsta.2019.0322>, 2020.

783 Kodros, J. K., Papanastasiou, D. K., Paglione, M., Masiol, M., Squizzato, S., Florou, K., Skyllakou, K., Kaltsonoudis, Ch.,
784 Nenes, A., and Pandis, S. N.: Rapid dark aging of biomass burning as an overlooked source of oxidized organic aerosol,
785 *Proc. Natl. Acad. Sci. USA*, 117, 33028–33033, <https://doi.org/10.1073/pnas.2010365117>, 2020.

786 Kurihara, K., Iwata, A., Murray Horwitz, S. G., Ogane, K., Sugioka, T., Matsuki, A., and Okuda, T.: Contribution of
787 physical and chemical properties to dithiothreitol-measured oxidative potentials of atmospheric aerosol particles at
788 urban and rural sites in Japan, *Atmosphere*, 13, 319, <https://doi.org/10.3390/atmos13020319>, 2022.

789 Künzli, N., Mudway, I. S., Gotschi, T., Shi, T. M., Kelly, F. J., Cook, S., Burney, P., Forsberg, B., Gauderman, J. W.,
790 Hazenkamp, M. E., Heinrich, J., Jarvis, D., Norback, D., Payo-Losa, F., Poli, A., Sunyer, J., and Borm, P. J. A.:
791 Comparison of oxidative properties, light absorbance, and total and elemental mass concentration of ambient PM_{2.5}
792 collected at 20 European sites, *Environ. Health Perspect.*, 114, 684–690, <https://doi.org/10.1289/ehp.8584>, 2006.

793 Lelieveld, J., Evans, J. S., Fnais, M., Giannadaki, D., Pozzer, A.: The contribution of outdoor air pollution sources to
794 premature mortality on a global scale, *Nature*, 525, 367–371, <https://doi.org/10.1038/nature15371>, 2015.

795 Lelieveld, J., Pozzer, A., Pöschl, U., Fnais, M., Haines, A., and Münzel, T.: Loss of life expectancy from air pollution
796 compared to other risk factors: a worldwide perspective, *Cardiovasc. Res.*, 116, 1910–1917,
797 <https://doi.org/10.1093/cvr/cvaa073>, 2020.

798 Lionetto, M. G., Guascito, M. R., Giordano, M. E., Caricato, R., De Bartolomeo, A. R., Romano, M. P., Conte, M., Dinovi,
799 A., and Contini, D.: Oxidative potential, cytotoxicity, and intracellular oxidative stress generating capacity of PM₁₀: a
800 case study in south of Italy, *Atmosphere*, 12, 464, <https://doi.org/10.3390/atmos12040464>, 2021.

801 Norris, G., Duvall, R., Brown, S., and Bai, S.: EPA Positive Matrix Factorization (PMF) 5.0 fundamentals and user guide,
802 Technical Report, U.S. Environmental Protection Agency, National Exposure Research Laboratory, Washington, USA,
803 2014.

804 Paatero, P. and Tapper, U.: Positive matrix factorization: A non-negative factor model with optimal utilization of error
805 estimates of data values, *Environmetrics*, 5, 111–126, <https://doi.org/10.1002/env.3170050203>, 1994.

806 Pye, H. O. T., Ward-Caviness, C. K., Murphy, B. N., Appel, K. W., and Seltzer, K. M.: Secondary organic aerosol
807 association with cardiorespiratory disease mortality in the United States, *Nat. Commun.*, 12, 7215,
808 <https://doi.org/10.1038/s41467-021-27484-1>, 2021.

809 Riediker, M., Zink, D., Kreyling, W., Oberdörster, G., Elder, A., Graham, U., Lynch, I., Duschl, A., Ichihara, G., Ichihara,
810 S., Kobayashi, T., Hisanaga, N., Umezawa, M., Cheng, T. J., Handy, R., Gulumian, M., Tinkle, S., and Cassee, F.:
811 Particle toxicology and health - where are we?, *Part. Fibre Toxicol.*, 16, 19, <https://doi.org/10.1186/s12989-019-0302-8>,
812 2019.

813 Salma, I., Chi, X., and Maenhaut, W.: Elemental and organic carbon in urban canyon and background environments in
814 Budapest, Hungary, *Atmos. Environ.*, 38, 27–36, <https://doi.org/10.1016/j.atmosenv.2003.09.047>, 2004.

815 Salma, I., Ocskay, R., Raes, N., and Maenhaut, W.: Fine structure of mass size distributions in urban environment, *Atmos.*
816 *Environ.*, 39, 5363–5374, <https://doi.org/10.1016/j.atmosenv.2005.05.021>, 2005.

817 ~~Salma, I. and Maenhaut, W.: Changes in chemical composition and mass of atmospheric aerosol pollution between 1996 and~~
818 ~~2002 in a Central European city, *Environ. Pollut.*, 143, 479–488, <https://doi.org/10.1016/j.envpol.2005.11.042>, 2006.~~

819 Salma, I., Németh, Z., Weidinger, T., Kovács, B., and Kristóf, G.: Measurement, growth types and shrinkage of newly
820 formed aerosol particles at an urban research platform, *Atmos. Chem. Phys.*, 16, 7837–7851,
821 <https://doi.org/10.5194/acp-16-7837-2016>, 2016.

822 Salma, I., Vasanits-Zsigrai, A., Machon, A., Varga, T., Major, I., Gergely, V., and Molnár, M.: Fossil fuel combustion,
823 biomass burning and biogenic sources of fine carbonaceous aerosol in the Carpathian Basin, *Atmos. Chem. Phys.*, 20,
824 4295–4312, <https://doi.org/10.5194/acp-20-4295-2020>, 2020a.

825 Salma, I., Vörösmarty, M., Gyöngyösi, A. Z., Thén, W., and Weidinger, T.: What can we learn about urban air quality with
826 regard to the first outbreak of the COVID-19 pandemic? A case study from central Europe, *Atmos. Chem. Phys.*, 20,
827 15725–15742, <https://doi.org/10.5194/acp-20-15725-2020>, 2020b.

828 Salma, I., Varga, P. T., Vasanits, A., Machon, A.: Secondary organic carbon and its contributions in different atmospheric
829 environments of a continental region and seasons, *Atmos. Res.*, 278, 106360,
830 <https://doi.org/10.1016/j.atmosres.2022.106360>, 2022.

831 Shahpoury, P., Zhang, Z. W., Arangio, A., Celo, V., Dabek-Zlotorzynska, E., Harner, T., and Nenes, A.: The influence of
832 chemical composition, aerosol acidity, and metal dissolution on the oxidative potential of fine particulate matter and
833 redox potential of the lung lining fluid, *Environ. Internat.*, 148, 106343, <https://doi.org/10.1016/j.envint.2020.106343>,
834 2021.

835 ~~Shahpoury, P., Zhang, Z. W., Filippi, A., Hildmann, S., Lelieveld, S., Mashtakov, B., Patel, B. R., Traub, A., Umbrio, D.,~~
836 ~~Wietzorek, M., Wilson, J., Berkemeier, T., Celo, V., Dabek-Zlotorzynska, E., Evans, G., Harner, T., Kerman, K.,~~
837 ~~Lammel, G., Nooroziifar, M., Pöschl, U., and Tong, H.: Inter-comparison of oxidative potential metrics for airborne~~
838 ~~particles identifies differences between acellular chemical assays, *Atmos. Pollut. Res.*, 13, 101596,~~
839 ~~<https://doi.org/10.1016/j.apr.2022.101596>, 2022.~~

840 Srivastava, D., Tomaz, S., Favez, O., Lanzafame, G. M., Golly, B., Besombes, J.-L., Alleman, L. Y., Jaffrezo, J.-L., Jacob,
841 V., Perraudin, E., Villenave, E., and Albinet, A.: Speciation of organic fraction does matter for source apportionment.
842 Part 1: A one-year campaign in Grenoble (France), *Sci. Total Environ.*, 624, 1598–1611,
843 <https://doi.org/10.1016/j.scitotenv.2017.12.135>, 2018.

844 Szigeti, T., Óvári, M., Dunster, C., Kelly, F. J., Lucarelli, F., and Záray, G.: Changes in chemical composition and oxidative
845 potential of urban PM(2.5) between 2010 and 2013 in Hungary, *Sci. Total Environ.*, 518–519, 534–544,
846 <https://doi.org/10.1016/j.scitotenv.2015.03.025>, 2015.

847 Valavanidis, A., Fiotakis, K., and Vlachogianni, T.: Airborne particulate matter and human health: toxicological assessment
848 and importance of size and composition of particles for oxidative damage and carcinogenic mechanisms, *J. Environ.*
849 *Sci. Health C*, 26, 339–362, <https://doi.org/10.1080/10590500802494538>, 2008.

850 Valavanidis, A., Vlachogianni, T., Fiotakis, K., and Loridas, S.: Pulmonary oxidative stress, inflammation and cancer:
851 respirable particulate matter, fibrous dusts and ozone as major causes of lung carcinogenesis through reactive oxygen
852 species mechanisms, *Int. J. Environ. Res. Public Health*, 10, 3886–3907, <https://doi.org/10.3390/ijerph10093886>, 2013.

853 Varga, G.: Changing nature of Saharan dust deposition in the Carpathian Basin (Central Europe): 40 years of identified
854 North African dust events (1979–2018), *Environ. Int.*, 139, 105712, <https://doi.org/10.1016/j.envint.2020.105712>,
855 2020.

856 Verma, V., Rico-Martinez, R., Kotra, N., King, L., Liu, J., Snell, T. W., and Weber, R. J.: Contribution of water-soluble and
857 insoluble components and their hydrophobic/hydrophilic subfractions to the reactive oxygen species-generating
858 potential of fine ambient aerosols, *Environ. Sci. Technol.*, 46, 11384–11392, <https://doi.org/10.1021/es302484r>, 2012

859 Verma, V., Fang, T., Guo, H., King, L., Bates, J. T., Peltier, R. E., Edgerton, E., Russell, A. G., and Weber, R. J.: Reactive
860 oxygen species associated with water-soluble PM_{2.5} in the southeastern United States: spatiotemporal trends and source
861 apportionment, *Atmos. Chem. Phys.*, 14, 12915–12930, <https://doi.org/10.5194/acp-14-12915-2014>, 2014.

862 Verma, V., Fang, T., Xu, L., Peltier, R. E., Russell, A. G., Ng, N. L., and Weber, R. J.: Organic aerosols associated with the
863 generation of reactive oxygen species (ROS) by water-soluble PM_{2.5}, *Environ. Sci. Technol.*, 49, 4646–4656,
864 <https://doi.org/10.1021/es505577w>, 2015.

865 Visentin, M., Pagnoni, A., Sarti, E., and Pietrogrande, M. C.: Urban PM_{2.5} oxidative potential: Importance of chemical
866 species and comparison of two spectrophotometric cell-free assays, *Environ. Pollut.*, 219, 72–79,
867 <https://doi.org/10.1016/j.envpol.2016.09.047>, 2016.

868 Wang, S., Ye, J., Soong, R., Wu, B., Yu, L., Simpson, A. J., and Chan, A. W. H.: Relationship between chemical
869 composition and oxidative potential of secondary organic aerosol from polycyclic aromatic hydrocarbons, *Atmos.*
870 *Chem. Phys.*, 18, 3987–4003, <https://doi.org/10.5194/acp-18-3987-2018>, 2018.

871 [Weichenthal, S., Shekarizfard, M., Traub, A., Kulka, R., Al-Rijleh, K., Anowar, S., Evans, G., and Hatzopoulou, M.:
872 Within-city spatial variations in multiple measures of PM_{2.5} oxidative potential in Toronto, Canada, *Environ. Sci.
873 Technol.*, 53, 2799–2810, <https://doi.org/10.1021/acs.est.8b05543>, 2019.](#)

874 Weber, S., Uzu, G., Calas, A., Chevrier, F., Besombes, J.-L., Charron, A., Salameh, D., Ježek, I., Močnik, G., and Jaffrezo,
875 J.-L.: An apportionment method for the oxidative potential of atmospheric particulate matter sources: application to a
876 one-year study in Chamonix, France, *Atmos. Chem. Phys.*, 18, 9617–9629, <https://doi.org/10.5194/acp-18-9617-2018>,
877 2018.

878 Weber, S., Uzu, G., Favez, O., Borlaza, L. J. S., Calas, A., Salameh, D., Chevrier, F., Allard, J., Besombes, J.-L., Albinet, A.,
879 Pontet, S., Mesbah, B., Gille, G., Zhang, S., Pallares, C., Leoz-Garziandia, E., and Jaffrezo, J.-L.: Source
880 apportionment of atmospheric PM₁₀ oxidative potential: synthesis of 15 year-round urban datasets in France, *Atmos.*
881 *Chem. Phys.*, 21, 11353–11378, <https://doi.org/10.5194/acp-21-11353-2021>, 2021.

882 Wong, J. P. S., Tsagkaraki, M., Tsiotra, I., Mihalopoulos, N., Violaki, K., Kanakidou, M., Sciare, J., Nenes, A., and Weber,
883 R. J.: Effects of atmospheric processing on the oxidative potential of biomass burning organic aerosols, *Environ. Sci.*
884 *Technol.*, 53, 6747–6756, <https://doi.org/10.1021/acs.est.9b01034>, 2019.

885 Yang, A., Hellack, B., Leseman, D., Brunekreef, B., Kuhlbusch, T. A., Cassee, F. R., Hoek, G., and Janssen, N. A.:
886 Temporal and spatial variation of the metal-related oxidative potential of PM_{2.5} and its relation to PM_{2.5} mass and
887 elemental composition, *Atmos. Environ.*, 102, 62–69, <https://doi.org/10.1016/j.atmosenv.2014.11.053>, 2015.

888 Yu, S., Liu, W., Xu, Y., Yi, K., Zhou, M., Tao, S., and Liu, W.: Characteristics and oxidative potential of atmospheric PM_{2.5}
889 in Beijing: Source apportionment and seasonal variation, *Sci. Total Environ.*, 650, 277–287,
890 <https://doi.org/10.1016/j.scitotenv.2018.09.021>, 2019.

891 Yue, Y., Chen, H., Setyan, A., Elser, M., Dietrich, M., Li, J., Zhang, T., Zhang, X., Zheng, Y., Wang, J., and Yao, M.: Size-
892 resolved endotoxin and oxidative potential of ambient particles in Beijing and Zürich, *Environ. Sci. Technol.*, 52,
893 6816–6824, <https://doi.org/10.1021/acs.est.8b01167>, 2018.

894 Zhang, Z.-H., Hartner, E., Utinger, B., Gfeller, B., Paul, A., Sklorz, M., Czech, H., Yang, B. X., Su, X. Y., Jakobi, G.,
895 Orasche, J., Schnelle-Kreis, J., Jeong, S., Gröger, T., Pardo, M., Hohaus, T., Adam, T., Kiendler-Scharr, A., Rudich, Y.,
896 Zimmermann, R., and Kalberer, M.: Are reactive oxygen species (ROS) a suitable metric to predict toxicity of
897 carbonaceous aerosol particles?, *Atmos. Chem. Phys.*, 22, 1793–1809, <https://doi.org/10.5194/acp-22-1793-2022>, 2022.